NON-DESTRUCTIVE TESTING OF THE PARTS MANUFACTURED BY DIRECT METAL LASER SINTERING

D. Kouprianoff[1*#], A. du Plessis[2], I. Yadroitsava[1], I. Yadroitsev[1]

[1]Department of Mechanical and Mechatronic Engineering, [1]Central University of Technology, South Africa
[2]University of Stellenbosch, CT Scanner Facility, Stellenbosch, South Africa

Poedel007.dk@gmail.com
anton2@sun.ac.za
iyadroitsava@cut.ac.za
iyadroitsau@cut.ac.za

ABSTRACT

Interest in Additive Manufacturing (AM) has grown considerably in the past decades. The industry has gained the great benefits from this type of technologies. The main advantages being geometrical freedom that allows designing parts with complex shape, which are difficult or impossible to produce by conventional technology, shortened design to product time, customization and possible use of several materials in one process. Direct Metal Laser Sintering (DMLS) is one of the most promising AM techniques that utilize metal materials. Due to the complex nature of the DMLS process, one of the drawbacks is the high residual stress in the manufactured parts. This can result to the formation of internal cracks and eventually to a substantial deterioration of the mechanical properties of the products and their application properties. For this reason it is very important to identify defective parts before enrolling into service. Non-destructive testing (NDT) is effective for detection of internal defects without causing damage. NDT also covers a wide group of methods of analysis used to evaluate the properties of a material. NDT techniques like ultrasonic inspection, acoustic emission, visual inspection, thermography, X-ray and 3D computed tomography (CT) inspection, etc. are now widely used for various industrial applications. For the detection of defects and to study the properties of the material each of these methods uses different physical principles that have their advantages and disadvantages. In this study some of the NDT techniques in terms of their applicability to the inspection of parts manufactured by DMLS technology are considered.

[#] The author is enrolled for an M Eng degree in the Department of Department of Mechanical and Mechatronic Engineering, University of Central University of Technology, Free state, South Africa

* Corresponding author

1. INTRODUCTION

Non-destructive testing (NDT) refers to the various techniques used to monitor the health of a material, component, or system in a structure without causing damage. NDT can detect potential failures as well as inform users of the appropriate time to replace their components according to the safety and performance. “As a result, NDT has become a highly valuable and critical technique in many precision industries, as it can save both money and time in product evaluation, troubleshooting, and research” [1].

1.1 Visual testing

Visual testing (VT) is the first methods used in NDT history. As the name implies this method makes use of an image to detect defects with the eye or light sensing device. VT has many applications in almost all industries. VT can be applied during production on finished parts and during service.

VT equipment makes use of visual aids such as microscopes to investigate the surface of a component. Table 1 shows the advantages and limitations of VT.

Table 1: VT advantages and limitations

Advantages	*Limitations*
Inexpensive	Only surface can be inspected
Minimal training required	Access necessary

Small surface defects like micro cracks are difficult to detect on DMLS produced components because of the irregular surface roughness of as-built components, this irregular surface is due to the partial sintering of surrounding powders, tracks formed by laser sintering and the layer wise building process of DMLS. It should be kept in mind that the build direction of the part influences the surface roughness. Visual detected defects of DMLS components are shown in Figs. 1 & 2. In Fig. 2a the SEM photographs clearly show partial sintering of the powder onto the part and the layers' boundaries can also be identified. A micro crack is indicated on the top surface in Fig. 2b. Surface finish is important in visual testing as it determines what kind and size of defect can be detected. Similar to conventional metal welding, in VT of DMLS parts it is important to know what is seen and to be able to identify the origin of the defect. Surface finish also influences mechanical fatigue. In fatigue cracking there are three stages, initial damage, crack propagation and failure due to cross-sectional reduction [2].

1.2 Radiographic testing

Radiographic testing (RT) are categorized in two ways: Firstly the way in which the data are extracted and secondly the type of radiation used. Conventional RT makes use of a radiographic film to record data whereas Computed Radiography (CR) makes use of electronic sensing device and computer software to interpret the data. The three types of radiation used in the different methods are: Neutron, X-ray and Gamma radiation. X-ray machines are categorized by energy groups [2–3].

RT can be applied to most materials, shapes and structures. Innovations such as Computed Tomography (CT) make this technology's applications ever expanding. In CT an object is exposed to collimated X-rays and the absorbed radiation is measured with a sensor on the opposite side. Any discontinuities will affect the exposure absorbed by the sensor. The procedure is repeated from different angles around the object until a 3D image can be reconstructed. A particular advantage of this CT is the ability to view cross sections at various depths in the sample [2, 6]. Table 2 shows the advantages and limitations of RT

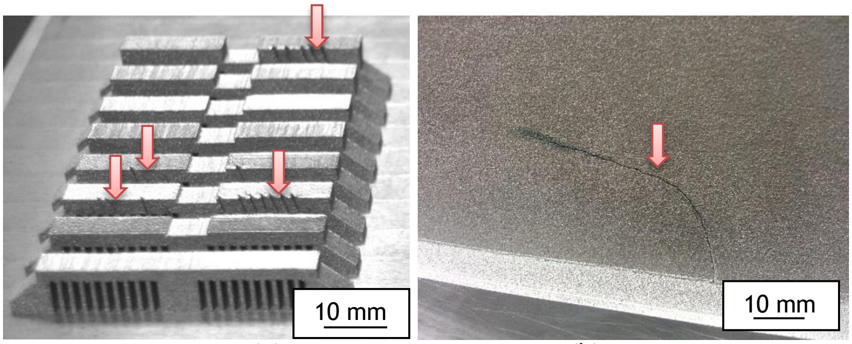

(a) (b)

Fig. 1. Defects of the DMLS samples (a) and macro-cracks (b).

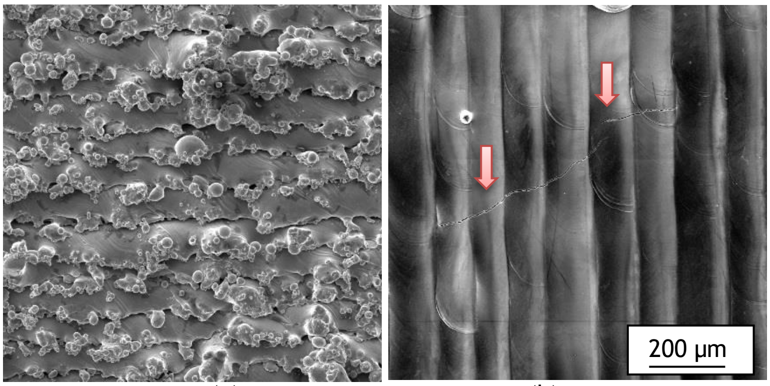

(a) (b)

Fig. 2. Surface of the cube DMLS samples: side surface (a) and top view with micro-cracks (b).

Table 2: RT advantages and limitations

Advantages	*Limitations*
Provides a permanent record	Limited thickness based on material density
High sensitivity	Orientation of planar discontinuities is crucial
Most widely used and accepted volumetric examination	Radiation hazard

MicroCT has been applied successfully in AM industry thus far and therefore was investigated and reported. MicroCT has a higher resolution than conventional CT. Du Pllessis et al. [5] found that pores in a Ti6Al4V DMLS produced cylindrical sample (60 mm high and 30 mm diameter build direction in the long axis) could be detected using MicroCT with a 48 and 25 µm resolution and confirmed their results after taking micrographs of a physical sectioning within their sample. They stated that these defects are difficult to detect with other means such as traditional radiographic testing, due to the size and geometry and complexity of the DMLS objects. This is because in conventional radiography a single scan through the object is used to produce a projection onto a film or sensor to reproduce a picture whereas in CT these scans are repeated at different angles around the object. These scans are then superimposed on each other to form a 3D model [5].

1.3 Ultrasonic testing

High frequency sound pulses from a transducer propagate through the test material, reflecting at interferences. Various techniques and equipment make this a very versatile solution. Regarding the selection of these techniques Hellier [2] states that the ways in which the sound waves propagate through the material and are attenuated, reflected or transmitted dictate the different ultrasonic methods or techniques used to detect the many types of discontinuities that can exist.

Ultrasonic testing (UT) can be used if sound transmission and surface finish are good and the shape is not complex. Table 3 shows the advantages and limitations of UT. A major innovation in UT is phased array inspection.

Table 3: UT advantages and limitations

Advantages	*Limitations*
Provides precise results quickly	No permanent record(usually)
Thickness and depth information	Material attenuation, surface finish and contour
Type of flaw can be obtained from one side of the component	Requires Couplant

1.4 Acoustic emission testing

Acoustic emission testing (AE) is based on the principle that elastic stress waves are generated by the rapid release of energy in the material due to relaxation of the stress and strain fields. These waves are then measured by electric sensors and interpreted. AE is used in on-line monitoring of pipes and pressure vessels, leak detection rotating equipment, production line components and structures subject to stress and loading [3].

Table 4: AE advantages and limitations

Advantages	*Limitations*
Large components (pipes etc.) can be monitored, less sensitive to geometry	Sensors often need contact with surface
Can possibly predict failure	Multiple sensors needed for flaw detection
Continuous monitoring(On-line)	Signal interpretation required

Another AE method that is used is based on the natural resonant frequency of a component. Resonant frequency of any component is dependent on the material properties, dimensions and densities. This resonant frequency is what gives different musical instruments their unique sound. For example string instruments sound different when the tension in the string is changed; the same applies for different diameters of the string or when using metal compared to nylon. Various different techniques from different companies exist; some of them are Resonant Acoustic method, Resonant Inspection Theory and Impulse Excitation Technique [6-8]. RFDA Basic from IMCE makes use of Impulse Excitation Technique; they also use this technology to measure elastic properties of predefined shapes. This is done quick and effectively by measuring the resonant frequencies and internal friction damping of the specimen. The RFDA Basic is designed for performing such tasks by tapping the component creating an impulse that causes the component to vibrate at its own natural frequency. These frequencies are measured by a microphone and sent to the RFDA software where the resonant frequencies and internal friction is measured and then elastic properties can be calculated [6]. This method is also used to look for defects on production lines of metal components. If the component being measured has a deviation from the known frequency of a faultless component it indicates that there is a structural defect within the measured component e.g., a crack that reduces the stiffness causing the resonant frequency to drop. Degree of shift of the resonant frequency is proportional to the degree of the defect. The resonant frequency is given by:

$$f_r = \sqrt{\frac{k}{m}}$$

where k and m are the stiffness and the mass of the material, respectively, which is dependent on material properties and sample geometry [3].

2. DMLS EVALUATION

In serial production and safety related components such as automotive and aeronautic applications detailed documentation of the part quality are becoming increasingly important Krauss et al. [9]. These documents can be obtained by different means including the manufacturing of ancillary test specimens or the non-destructive testing using computer tomography. Another option is to monitor the process during building. This can be done due to the layer-wise build up process of additive manufacturing which allows for detailed monitoring. DMLS objects consist of a set of individual single layers and tracks. The primary units for DMLS are single tracks, their combination creates a single layer, and from the sequence of layers, a 3D object is sintered. To produce fully dense objects from the employed powder material, optimal process parameters and a specific strategy of manufacturing should be used [10]. The major concerns in DMLS are high roughness, porosity and residual stress.

Visual defects can be detected only after cleaning the sample from the powder material (Fig. 1), it can be problems with accuracy (Fig. 1a) or macro cracks (Fig. 1b). Online system for monitoring the quality is the main problem now for DMLS technology. Surface roughness of DMLS samples depend on strategy of building and scanning process, layer thickness and process parameters (Fig. 2).

Residual stress can have both undesirable and desirable effects on the material properties. It is a known fact that residual stress occurs in every existing material. The amount of residual stress formation in a material varies due to the following three factors: the type of material, material processing and the material loads [11]. In DMLS parts, tensile residual stress is a concern because it could cause part distortion, cracks and reduce the strength of the part [12]. Micro-cracks for the sample from Ti–Al alloy is shown in Fig. 2b.

The mechanism of distortion, irregularities and balling effect are associated with thermo-physical properties of materials; granulo-morphometric characteristics of the powder and inhomogeneity in powder layer thickness; energy input parameters including laser power, spot size and scanning speed; melt hydrodynamics, etc. The density of DMLS parts remain a huge concern as it directly affects the mechanical properties. At optimal process-parameters, porosity in DMLS is very low and typical size of the pores is less than 150 μm (Fig. 3).

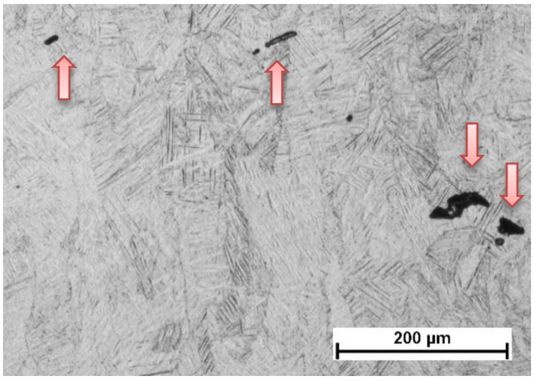

Fig. 3. Cross-section of DMLS Ti6Al4V (ELI) alloy.

3. MATERIALS AND METHODS

Ti6Al4V (ELI) powder was pre-alloyed gas atomized powder. The chemical composition was as follows: Ti – balance, Al – 6,34%, V – 3,94%, O – 0,082%, N – 0.006%, H – 0,001%, Fe – 0,25%, C – 0.006% (weight %). The equivalent diameters (by volume) of the powder particles were d_{10} = 12.03 µm, d_{50} = 21.38 µm and d_{90} = 31.15 µm.

Ti6Al4V samples were produced with the following process parameters: Laser power of 170 W, scanning speed of 1.25 ms^{-1}, layer thickness of 30 µm and argon was used as the protective atmosphere. A back-and-forth (zigzag) scanning strategy by strips with width of 5 mm and the hatch distance between tracks of 100 µm was applied for manufacturing rectangular specimens (60x20x7 mm). 10 samples were manufactured, 6 without defects and 4 with artificial defects. The artificial defect with prescribed CAD sizes of 40x10x0.090 mm was placed in the centre of the rectangle. 5 blocks (3 without defects and 2 with defects) have been separated from the substrate by wire cutter. The other 5 remaining samples were subjected to heat treatment (650°C, 3 hours) for stress relieving, after which it was removed.

Visual testing (VT) of the surface was done using Scanning electron microscopy (SEM) and was carried out with NeoScope JCM 5000 operated at 15 kV.

The surface roughness was measured using a Mitutoyo SJ-210; a portable surface roughness meter that fulfills ISO 1997 requirements. The parameters used for the measurements are as follows: distance of measurement 5 mm; speed of detector 0.5 mm/s.

X-ray micro computed tomography (microCT) was used in this study. A General Electric Phoenix V|Tome|X L240/NF180 was used. For all specimens the X-ray settings were 150 kV and 150 µA, 2000 images were acquired in a full rotation at image acquisition time of 500 ms per image, with average 2 images and one image skip per rotation. Detector shift was activated to minimize ring artefacts. Background calibration was performed and the scan time was approximately 40 minutes per scan at 40 µm voxel size. Reconstruction was done with system-supplied Datos reconstruction software. Analysis was performed with Volume Graphics VGStudio Max 2.1 or Visualization Sciences Group Avizo Fire 8.0 commercial 3D analysis software packages.

To determine the resonant frequencies, impulse excitation measurements were made with the RFDA Basic hardware and software from IMCE in an air atmosphere at room temperature.

4. RESULTS AND DISCUSSION

Visual inspection of manufactured Ti6Al4V samples did not reveal any visible defects and cracks on the surfaces. The surface roughness influences the size of the defect that can be detected. The surface roughness of the DMLS specimen varies with the direction in which the probe moves with regard to the building direction or the scanning strategy used with the specimen. For example, when checking the top surface of the specimen if the probe moves perpendicular to the tracks it will have a greater roughness than when it is running on a track in the same direction of scanning. Roughness measurements were made 12 times on each surface each time rotating the block by some degree. The top surface roughness was recorded as *Rz*=34.5 µm, *Ra*=5.9 µm average with 12.97 µm and 1.79 µm standard deviation respectively. The side surface roughness was recorded as *Rz*=89.9 µm, *Ra*=14.5 µm average with 17.93 µm and 3.19 µm standard deviation respectively. The large standard deviation can be attributed to the factors that were mentioned above. The probability that small defects like micro cracks can be detected on the side surface with Rz=89.9 µm is much less than compared to the top surface (*Rz*=34.5 µm).

For the study of presence of internal defects, X-ray micro computed tomography has been applied. In order to eliminate any edge noise effects, sub-surface by 4 voxels was excluded from the analysis at 3D image processing. The control group of samples (as-built (AB) 1-3 and stress relieved (SR) 1-3) had no defects, only some random small pores. The samples AB4 and SR4 had a very fine defect layer, while samples AB5 and SR5 had a more pronounced defect layer, but it was not continuous (Fig. 4). The porosity of the samples with artificial defects was planned near 0.5 %, but in reality, the estimated from CT scans porosity of the samples was much lower: 0%, 0.06% and 0.11% for AB1, AB4 and AB5 samples (Fig. 5a) and 0%, 0.03% and 0.31% for SR1, SR4 and SR5 specimens (Fig. 5b). The partial remelting of the powder in the inner area of the sample (artificial defect) can cause the porosity reduction. Some of the unmelted powder, which remains in the inner cavities, can mask the pores when using microCT (Fig. 6).

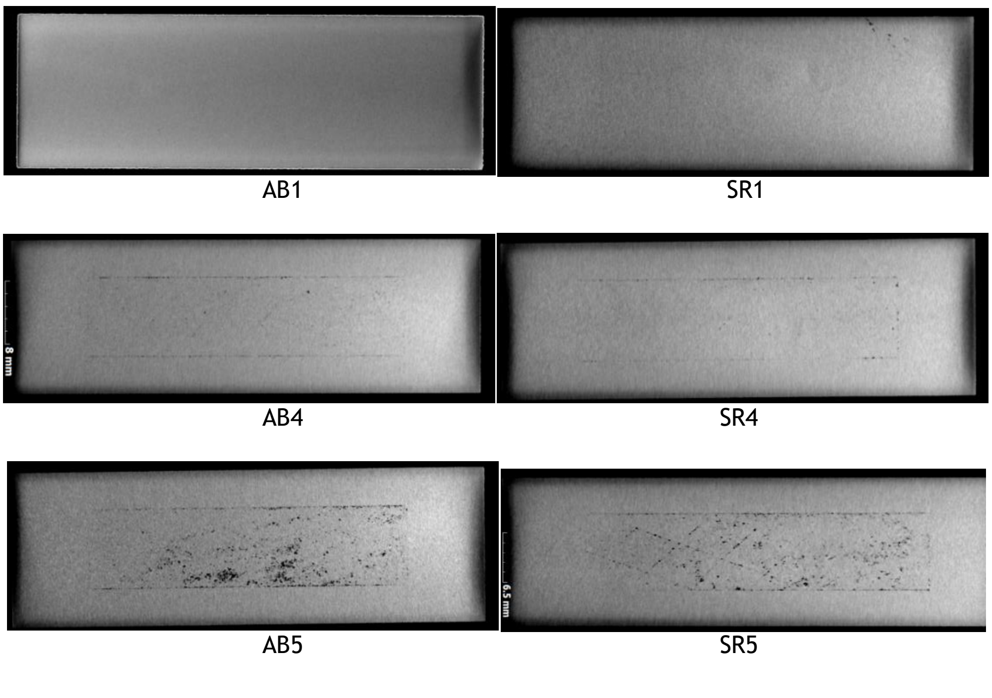

Fig. 4. DMLS samples without defects and with artificial defects upon microCT inspection (top view). AB – as-built samples, SR – stress relieved samples

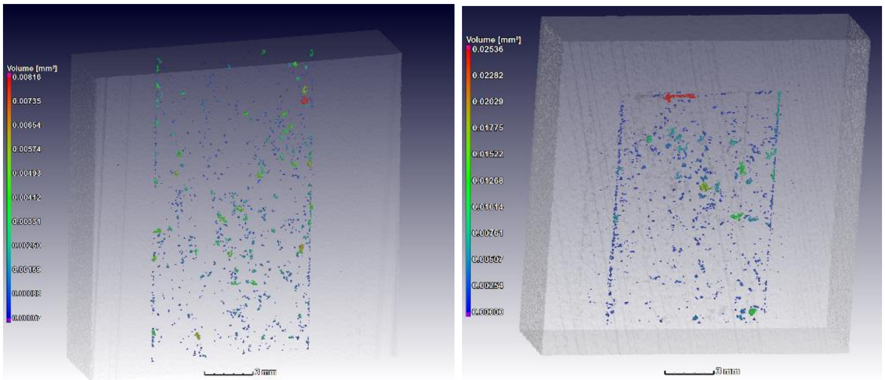

(a) (b)

Fig. 5. 3D distribution of the pores in the sub-volume near defects from a close-up 15 μm resolution at microCT inspection: AB5 (a) and SR5 (b) samples.

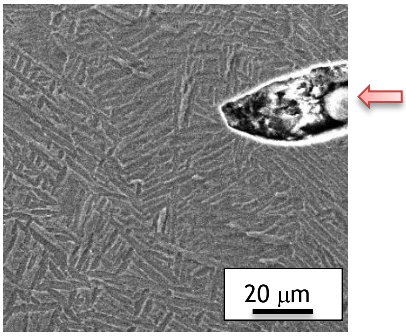

Fig. 6. Un-melted powder in the pores of a DMLS sample.

Acoustic emission testing (AE) based on measurements by RFDA Basic (IMCE) has shown that there are reliable differences in the data for the DMLS samples with different mass and thickness (Table 5, Fig. 7). Some noticeable differences in the frequencies were found between as-built and stress-relieved samples without defects: flexural and torsion frequencies were higher for stress relieved samples with similar mass.

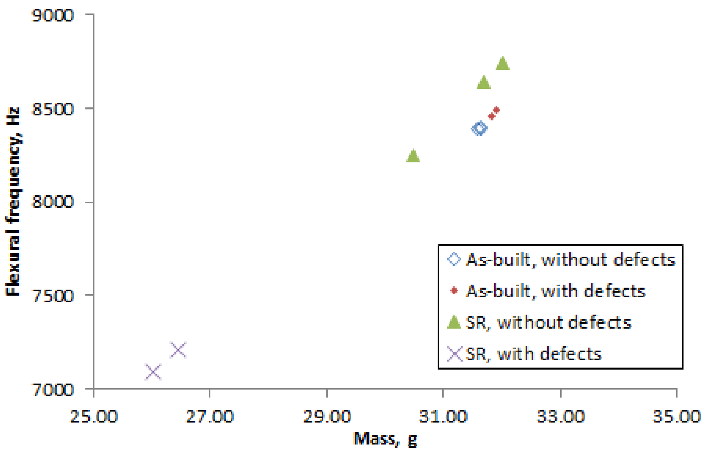

(a)

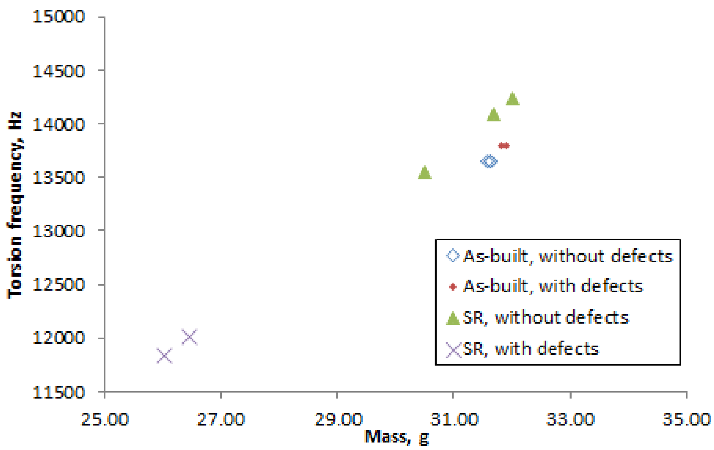

(b)

Fig. 7. Flexural (a) and torsional (b) frequencies of the different specimens *versus* the mass.

The RFDA Basic was able to calculate the modulus of elasticity and obtained the values of 107.1 GPa for as-built and to 111.9 GPa for stress relieved with a standard deviation of 0.5 GPa and 1.2 GPa respectively. The significant differences that were obtained between as-built and stress relieved samples are due to the stiffness that changed after stress relieving [13]. The mass has a direct effect on the frequency of the components. In Table 5 the mass can be compared to the shape of the sample flexural frequency and a clear relationship can be seen although mass is not the only contributing factor in the measured frequency. Unfortunately, the samples with defects were different in thickness and also in mass (Table 5). This does not give confidence to assert that as-built samples with defects had higher flexural and torsion frequencies due to the presence of the defect in the samples (Fig. 7). The mass of the SR4 and SR5 defected parts were much less than the other samples due to difference in thickness and they show to what extent the frequency can change with a relatively small change in mass.

Table 5: Acoustic emission testing data, sizes and mass of the samples

Sample	E-modulus, GPa*	Flexural Frequency,* Hz	Torsion frequency,* Hz	Length, mm	Width, mm	Thickness, mm	Mass, g
AB 1	106.55±0.022	8399.9±0.82	13649.9±0.39	60.15	19.93	6.15	31.64
AB 2	107.14±0.005	8390.0±0.20	13648.3±0.16	60.16	19.93	6.13	31.58
AB 3	106.95±0.009	8392.8±0.34	13643.5±0.05	60.18	19.95	6.14	31.65
AB 4	107.80±0.004	8487.0±0.19	13789.6±0.11	60.18	19.93	6.19	31.9
AB 5	106.86±0.318	8460.5±0.09	13791.3±0.13	60.18	19.93	6.19	31.83
SR 1	112.17±0.004	8244.2±0.19	13546.8±0.43	60.39	19.93	5.91	30.5
SR 2	112.85±0.005	8745.3±0.12	14240.0±0.05	60.19	19.92	6.23	32.01
SR 3	113.20±0.004	8644.4±0.08	14085.5±0.08	60.19	19.94	6.15	31.7
SR 4	111.12±0.008	7208.3±0.20	12014.8±0.15	60.45	19.93	5.15	26.47
SR 5	110.28±0.013	7090.4±0.45	11835.5±0.15	60.5	19.93	5.08	26.03

* Average value ± Standard deviation

5. CONCLUSION

The present study showed that even a relatively simple method such as RFDA Basic can identify the defective samples with low porosity (less than 0.5 percent) from the defect-free if the samples will have the same geometry. Differences between as-built and stress relieved samples could be detected. The RFDA Basic can potentially determine a “fingerprint” of frequencies for complex DMLS parts. This study has a perspective from the point of view of developing of a simple and effective method of determining defective

DMLS samples, as microCT is quite expensive and a time consuming method. Micro CT showed the ability to indicate the size, shape and position of a defect. The AE method showed the possibility to be a quick and inexpensive option to check quality of production DMLS parts.

6. ACKNOWLEDGEMENTS

This work is based on the research supported by the South African Research Chairs Initiative of the Department of Science and Technology and National Research Foundation of South Africa (Grant №97994) and the Collaborative Program in Additive Manufacturing (Contract №CSIR-NLC-CPAM-15-MOA-CUT-01). The authors are grateful to IMCE for carrying out the impulse excitation measurements.

7. REFERENCE

[1] **Chen, X.,** 2014. Computational and experimental approach for non-destructive testing by laser shearograph, Degree of Master of Science in Mechanical Engineering. Worcester Polytechnic Institute.

[2] **Hellier, C.J.,** 2012. *Handbook of nondestructive evaluation*, Mcgraw-Hill, USA.

[3] **Raj, B., Jayakumar,T., Thavasimuthu, M.**, 2007. *Practical non-destructive testing*, Alpha Science, India.

[4] **Central Analytical Facilities Sun** (Analytical Service). CT Scanner - Information. (Online) Available from Http://Academic.Sun.Ac.Za/Saf/Services/Services8.Html (Accessed July 7, 2016).

[5] **Du Plessis, A. Le Roux, Sg. Els, J, Booysen, G. Blaine, Dc.** 2015. Application of microct to the non-destructive testing of an additive manufactured titanium component. *Case Studies in Nondestructive Testing And Evaluation* 4, September, pp 1-7.

[6] **Imce Theory** (Online) Available from Imce Http://Www.Imce.Net/Theory (Accessed July 8, 2016).

[7] **Ndt-Inspection N.D.**, Resonant inspection theory, (**Online**) Available from: Http://Www.Ndt-Inspection.Com/Nutek/Technology.Htm (Accessed 7 July, 2016).

[8] **The modal shop, resonant acoustic method**, (Online) Available From: Http://Www.Modalshop.Com/Ndt/Resonant-Acoustic-Method?Id=73 (Accessed 21 July, 2016).

[9] **Krauss H, C. Eschey C., And Zaeh M.F.** 2014. Thermography for monitoring the selective laser melting process, *Physics Procedia*, 56, pp 64-67.

[10] **The modal shop , Technical Paper Archive**, N.D, Effect of Crack Size On Natural Frequency Using Resonant Inspection. (Online) Available From: Http://Www.Modalshop.Com/Ndt/Ndt-Ram-Technical-Paper-Archive?Id=754 (Accessed 21 July, 2016).

[11] **Hauk, V.**, 1997. *Structural and residual stress analysis by nondestructive methods*. Elsevier.

[12] **Kruth, J-P. Badrossamay, M. Yasa, E. Deckers, J. Thijs, L. Van Humbeeck, J.,** 2010. Part and material properties in selective laser melting of metals. In *Proceedings of the 16th international symposium on electromachining*.

[13] **Krakhmalev, P., Fredriksson, G., Yadroitsava I., Kazantseva N., du Plessis, A., Yadroitsev, I.**, 2016. Deformation behavior and microstructure of Ti6Al4V manufactured by SLM. *Physics Procedia*, 83, 778 – 788